



Published in final edited form as:

Ophthalmology. 2021 October ; 128(10): 1426–1437. doi:10.1016/j.ophtha.2021.03.036.

Optical Coherence Tomography Angiography Artifacts in Glaucoma

Alireza Kamalipour, MD¹, Sasan Moghimi, MD¹, Huiyuan Hou, MD, PhD¹, Rafaella C. Penteado, MD¹, Won Hyuk Oh, MD¹, James A. Proudfoot, MSc¹, Nevin El-Nimri, PhD¹, Eren Ekici, MD¹, Jasmin Rezapour, MD¹, Linda M. Zangwill, PhD¹, Christopher Bowd, PhD¹, Robert N. Weinreb, MD¹

¹Hamilton Glaucoma Center, Shiley Eye Institute, Viterbi Family Department of Ophthalmology, University of California San Diego, La Jolla, CA.

Abstract

Purpose: To determine the prevalence of different types of artifacts seen in optical coherence tomography angiography (OCTA) images of healthy and glaucoma eyes and to evaluate the characteristics associated with the increased likelihood of obtaining poor quality images.

Design: Retrospective study.

Participants: A total of 649 eyes of 368 healthy, glaucoma suspect, and glaucoma patients.

Methods: Angiogram high density (HD) and non-HD optic nerve head and macula OCTA images of participants were evaluated by 4 expert reviewers for the presence of different artifacts including eye movement, defocus, shadow, decentration, segmentation error, blink and Z offset in the superficial vascular layer. Each OCTA scan was designated to have good or poor quality based on the presence of artifacts. The association of demographic and ocular characteristics with the likelihood of obtaining poor quality OCTA images was evaluated using generalized linear mixed model.

Correspondence: Robert N. Weinreb, MD, Shiley Eye Institute, University of California, San Diego, 9500 Gilman Drive, La Jolla, CA 92093-0946. rweinreb@ucsd.edu.

Commercial Disclosures:

1. Alireza Kamalipour: none
2. Sasan Moghimi: none
3. Huiyuan Hou: none
4. Rafaella C. Penteado: none
5. Won Hyuk Oh: none
6. James A. Proudfoot: none
7. Nevin El-Nimri: none
8. Eren Ekici: none
9. Jasmin Rezapour: none
10. Linda M. Zangwill: Research support—Carl Zeiss Meditec, Heidelberg Engineering, National Eye Institute, Topcon, and Optovue;
11. Christopher Bowd: none
12. Robert N. Weinreb: Financial support- National Eye Institute, Carl Zeiss Meditec, Centervue, Heidelberg Engineering, Konan, Optovue, Bausch & Lomb, Topcon; Consultant- Aerie Pharmaceuticals, Allergan, Bausch & Lomb, Eyeovia, Nicox, Novartis, Topcon; Patent- Toromedes, Carl Zeiss Meditec.

Publisher's Disclaimer: This is a PDF file of an unedited manuscript that has been accepted for publication. As a service to our customers we are providing this early version of the manuscript. The manuscript will undergo copyediting, typesetting, and review of the resulting proof before it is published in its final form. Please note that during the production process errors may be discovered which could affect the content, and all legal disclaimers that apply to the journal pertain.

Main Outcome Measures: The prevalence of OCTA artifacts and the factors associated with increased likelihood of capturing poor quality OCTA images.

Results: 5263 OCTA images were evaluated. Overall, 33.9% of the OCTA images had poor quality. The majority of images with acceptable quality scores (QS \geq 4) had no artifacts (76.6%). Other images had one (13.6%) or two or more artifacts (9.8%). Older age (P<0.001), male gender (P=0.045), worse visual field mean deviation (P<0.001), absence of eye tracking (P<0.001) and macular scan area (P < 0.001) were associated with a higher likelihood of obtaining poor quality images. In images with acceptable QS, the commercially available quality measures including QS and signal strength index had the area under the receiver operating characteristic curves of 0.65 (95% CI: 0.62, 0.69) and 0.70 (95% CI: 0.68, 0.73) to detect good quality images, respectively.

Conclusions: OCTA artifacts associated with poor quality images are frequent, and their prevalence is affected by ocular and patient characteristics. One should not rely solely on the quantitative assessments that are provided automatically by OCTA instruments. A systematic scan review should be conducted to ensure appropriate interpretation of OCTA images. Given the high prevalence of poor quality OCTA images, the images should be reacquired whenever an apparent and correctable artifact is present on a captured image.

Precis

This cross-sectional study on more than 5000 OCTA images showed that artifacts affecting the reliability of OCTA images are frequent. Also, their prevalence is affected by ocular and patient characteristics besides technical measurement related factors.

Keywords

optical coherence tomography angiography; artifact; glaucoma

Introduction

The recent introduction of optical coherence tomography angiography (OCTA) in ocular imaging has had a transformative role in providing qualitative and quantitative evaluation of the posterior segment of the eye. The ease of performing a dye free and non-invasive high resolution assessment of retinal microvasculature to discern different layers of retinal microvasculature provides advantages over traditional fluorescein and indocyanine green angiography.¹

Investigators have used OCTA imaging to assist in the evaluation of different ocular pathologies including glaucoma, age related macular degeneration, diabetic retinopathy, retinal vascular occlusions and choroidal neovascularization.^{2, 3} Previous studies of the retinal microvasculature have identified global and regional alterations in vessel density of glaucoma eyes compared to healthy eyes.^{4, 5} Moreover, vessel density has been shown to be decreased in the unaffected hemiretina of the eyes with single hemifield visual field defects.⁶ Further, decreased vessel density is significantly associated with the severity of visual field damage in primary open angle glaucoma⁷ and has the potential to serve as biomarkers of glaucoma progression.⁸

OCTA is a functional extension of optical coherence tomography (OCT) imaging that repeatedly scans each retinal region to differentiate static from dynamic structures.^{2,9} The overall imaging capability of OCTA technology is bound by the constraints seen in OCT images⁹. Different types of artifacts in OCT imaging, such as motion, decentration, cut edge, and retinal layer segmentation artifacts have been described previously that may affect the validity and interpretability of quantitative OCT measurements.^{10–14} The overall prevalence of artifacts has been as high as 38% in RTVue, 44% in Cirrus, and 53% in Topcon 3D OCT images obtained from eyes without apparent retinal pathologies.^{13, 15–17} These studies showed that sole reliance on the instrument provided measurements without the evaluation of OCT images can lead to erroneous interpretation of the data and this problem is even more pronounced in evaluating diseased ocular conditions.^{13, 15–17}

Most of the studies evaluating the quality of OCTA images have focused on the repeatability of the quantitative outputs of the device such as vessel density and foveal avascular zone area.^{18–21} Only a few studies have evaluated the prevalence of OCTA artifacts in images of healthy and diseased eye conditions, and they showed a substantial variation (from 9% to 53.5%) in the prevalence of artifacts leading to poor quality images.^{21–23} The potential implications of OCTA artifacts on the quality of these images is left unaddressed to a great extent in the existing literature. This is even a more pronounced problem in glaucoma since there have been no studies to address this issue. Moreover, ocular, patient and technical factors associated with OCTA artifacts are not well understood. The purpose of this study is to characterize the artifacts present in different types of OCTA images and determine their associated factors in a representative sample of more than 5,000 OCTA images from healthy subjects, glaucoma suspects and glaucoma patients.

Methods

This is a retrospective study of healthy subjects, glaucoma suspect and glaucoma patients who were enrolled in Diagnostic Innovations in Glaucoma Study (DIGS).²⁴ DIGS is an ongoing prospective longitudinal study designed to evaluate optic nerve structure and visual function in glaucoma. Study protocol adhered to the tenets of the declaration of Helsinki and was approved by the institutional review board of the University of California, San Diego (UCSD). Written informed consent was obtained from all study participants and the methods were in accordance with the Health Insurance Portability and Accountability Act (HIPPA).

Details of the DIGS protocols and eligibility have been described previously.²⁵ In brief, patients who were 18 years or older and had best-corrected visual acuity 20/40 at study entry underwent an annual comprehensive ophthalmologic examination, including review of medical history, best-corrected visual acuity, slit-lamp biomicroscopy, intraocular pressure (IOP) measurement with Goldmann applanation tonometry, gonioscopy, dilated fundus examination, stereoscopic optic disc photography (Nidek 3Dx Stereo Camera [Nidek Inc, Palo Alto, CA] after maximal pupil dilation), and ultrasound pachymetry for central corneal thickness (CCT; DGH Technology, Inc., Exton, PA) measurements in both eyes. The semiannual examination included intraocular pressure (IOP), OCTA imaging, spectral-domain OCT (SD-OCT) imaging, and 24–2 visual field (VF) testing. Eyes of the participants were categorized into healthy, glaucoma suspect and glaucoma. Healthy eyes

were those with IOP < 21 mmHg, absent history of elevated IOP, normal appearing optic disc and neuroretinal rim based on masked review of stereoscopic fundus photographs, and at least two reliable (fixation losses 33%, false negatives 33% and false positives 33%) normal VF tests. Those with IOP 22 mmHg, or evidence of glaucomatous optic neuropathy on fundus photograph evaluation, but without abnormal VF tests were classified as glaucoma suspects. Glaucoma eyes had two reliable and repeatable abnormal VF tests. Abnormal VF test was defined as a pattern standard deviation (PSD) outside of 95% confidence interval (CI) for the normal range or glaucoma hemifield test result of outside normal limits. Severity of glaucoma was assessed using VF mean deviation (MD). Eyes with previous history of surgery (unless having uncomplicated cataract or glaucoma surgery), uveitis, trauma, axial length more than 26 mm and evidence of non-glaucomatous optic neuropathy or retinal pathology other than glaucoma on fundus photograph and OCTA image evaluation were excluded from this study.

OCTA imaging protocols

The Avanti Angiovue system (Optovue Inc.) was used to acquire the images. This device is composed of a combined OCTA and SD-OCT system and provides a non-invasive three-dimensional visualization of the retinal microvasculature. In brief, it calculates motion contrast using the decorrelation signal generated from the consecutive scans of the same retinal area attributable to the dynamic structures. The method by which the device software translates the initial tissue reflectance recordings into the flow signals is called split-spectrum amplitude decorrelation angiography (SSADA) and has been described previously in detail.²⁶ OCTA images captured using this device can be divided into categories of high density (HD) and non-HD images based on the resolution. Non-HD images are composed of 304 A-scans in each B-scan and 304 B-scans over the whole cube area. HD images consist 400-A scans in each B-scan and 400-B scans over the entire cube area. Separate volumetric scans in a horizontal and vertical direction are obtained and translated to produce one final volumetric OCTA scan.

OCTA images of both the macula and optic nerve head (ONH) were included in this study. Macular images were centered over cross-sectional areas of 3X3 and 6X6 mm². ONH images were obtained over an area of 4.5X4.5 mm² with ONH being in the center. Thus, final scan types for the analysis included non-HD macular 3X3 mm², non-HD macular 6X6 mm², HD macular 6X6 mm², non-HD ONH 4.5X4.5 mm² and HD ONH 4.5X4.5 mm² images.

Staff performing the OCTA imaging underwent extensive training on how to obtain and evaluate the quality of OCTA images. Images were captured in a dark room after the process was fully introduced to the participants. The participants used eye patches to cover one eye during scan capture. Four trained observers (H.H, S.M, R.C.P, and A.K) evaluated the images to determine their qualification for further qualitative and quantitative use. Consensus meetings of the reviewers determined the qualification of images in case of disagreement. Images were determined to have poor quality if the automated image quality score (QS) generated by the software was less than 4 or any severe artifacts were present on the en-face angiogram. Presence of artifacts was evaluated in the images only if the

scan had the minimum QS of 4. According to previous evidence on the importance of superficial vascular layer on glaucoma diagnosis and progression,^{8, 27, 28} images of this layer were evaluated for quality and presence of severe artifacts. Superficial vascular layer in the macula was defined as a slab extending from the internal limiting membrane (ILM) to 10 μm below the inner plexiform layer. The ONH superficial vascular layer referred to the layer containing radial peripapillary capillary (RPC) vascular network that extends from the ILM to the posterior boundary of retinal nerve fiber layer (RNFL).

Definition of Artifacts

Common OCTA artifacts previously described^{9, 21–23} were evaluated including eye movement, defocus, shadow, decentration, segmentation error, blink and Z offset. Severity of each type of artifact was defined based on the relative proportion of the affected en-face area by that type of artifact to the whole en-face angiogram area. In brief, artifacts were considered as severe when they affected more than 10% of the total B-scans comprising the en-face angiogram for eye movement, decentration, defocus, shadow, and segmentation error artifacts and 5% of the total B-scans comprising the en-face angiogram for blink, and Z offset artifacts. (Table 1) Figure 1 illustrates representative artifacts of different type including eye movement, decentration, defocus, shadow, blink, and Z offset artifacts. Projection artifact is another common OCTA artifact previously described.^{9, 29} Since this artifact results from the shadow of vessels in the superficial layer on the deep layer microvasculature,^{9, 29} it is not present in the images of superficial vascular layer, and it was not evaluated in the current study.

Statistical Analysis

Continuous and categorical variables were reported as mean (95% CI) and number (percentage), respectively. The prevalence of each type of artifact according to different image types and as a whole was reported. Generalized linear mixed model was used to compare characteristics of good quality and poor quality images. Two independent random intercepts were included in the model for subject and eye (as a nested variable under subject category) to try to capture inter-subject and inter-eye correlations. Continuous variables were separately analyzed to check the linearity assumption before being included the models. Univariable and multivariable generalized linear mixed models were used to determine the association between several individual factors (including demographics, ocular parameters, image type and implementation of eye tracking) and the likelihood of capturing poor quality OCTA images. Variables with P-value < 0.1 in the univariable analysis and clinical independence were used to build the final model for the multivariable analysis.

To evaluate the effect of severe artifacts on global vessel density measurements of OCTA images, a subset of OCTA images acquired from the same eye at the same visit was included in a sub-analysis. For these images to be included, a pair including one poor quality and one good quality image needed to be available in the same visit. The variation in global vessel density measurements (superficial vessel density in the macular area and whole image peripapillary capillary density at the ONH area) between these pairs was evaluated and expressed as percentage of variation. Percentage of variation was defined as the absolute difference between the global metrics of the pair divided by the global metric of the good

quality image. Diagnostic accuracy of the automated quality measures provided by the OCTA software [QS and signal strength index (SSI)] to determine good quality OCTA images were evaluated in images with acceptable QS (for this study defined as QS ≥ 4) using receiver operating characteristic (ROC) curves. In addition, sensitivity analysis was done including OCTA images with acceptable QS to determine the sensitivity and specificity of different levels of QS and SSI to detect good quality images. Statistical analysis was performed using Stata software version 15.1 (StataCorp, College Station, TX). P-value < 0.05 was considered as statistically significant.

Results

Participants

A total of 5,263 OCTA images from 116 eyes of 63 healthy subjects, 165 eyes of 61 glaucoma suspect patients and 368 eyes of 244 glaucoma patients were included. The mean age of participants at the initial visit was 69.1 (67.7, 70.5) years and the majority were females (55.4%).

The demographics and ophthalmic characteristics of the three diagnostic groups are summarized in Table 2. Glaucoma eyes had older age ($P < 0.001$), lower baseline IOP ($P < 0.001$), worse MD ($P < 0.001$), higher PSD ($P < 0.001$) and higher cylindrical refractive error ($P < 0.001$) compared to eyes classified as glaucoma suspect and normal. Race distribution, CCT and axial length were not different among the diagnostic groups ($P = 0.106, 0.517$ and 0.935 , respectively). Three by three mm² non-HD macular image was the most common image type ($n = 1457, 27.7\%$) followed by non-HD ONH ($n = 1379, 26.2\%$), 6X6 mm² non-HD macula ($n = 896, 17.0\%$), HD macula ($n = 770, 14.6\%$) and HD ONH ($n = 761, 14.5\%$). The proportions of images taken with and without eye tracking technology is shown in Supplemental Table 1. The majority of images were taken from the eyes diagnosed with glaucoma ($n = 3280, 62.3\%$) followed by glaucoma suspect ($n = 1320, 25.1\%$) and healthy eyes ($n = 663, 12.6\%$).

Differences between good quality and poor quality images

A total of 33.9% (1785 out of 5263) of OCTA images had poor quality. This proportion was highest in 3X3 mm² non-HD macular images (44.4%), followed by 6X6 mm² non-HD macula images (32.1%), HD macular images (32.1%), non-HD ONH images (28.7%) and HD ONH images (27.2%). In addition, this proportion varied among different diagnostic subgroups from 16.4% (109 out of 663) in images captured from healthy eyes to 41.1% (1348 out of 3280) in images captured from glaucoma eyes. (Table 3)

Younger age at the time of scan acquisition ($P < 0.001$), higher IOP ($P = 0.042$), thicker CCT ($P = 0.008$), better MD ($P < 0.001$), lower PSD ($P < 0.001$), lower cylindrical refractive error ($P = 0.002$), higher image QS ($P < 0.001$) and SSI ($P < 0.001$) were observed in good quality images when compared to those with poor quality. Male to female ratio was higher in poor quality images ($P = 0.037$). Moreover, a greater proportion of images in the poor quality group were taken from glaucoma eyes compared to that proportion in the good quality group ($P < 0.001$) [Table 3].

Results of the univariable analysis showed that higher likelihood of capturing a poor quality OCTA image was significantly associated with older age ($P < 0.001$), male gender ($P = 0.037$), lower IOP ($P = 0.042$), lower CCT ($P = 0.008$), worse MD ($P < 0.001$), higher PSD ($P < 0.001$), higher cylindrical refractive error ($P = 0.002$), diagnosis ($P < 0.001$), absence of eye tracking technology ($P < 0.001$), and image type ($P < 0.001$). Race, axial length, spherical refractive error and spherical equivalent of refraction did not show a significant association with the likelihood of obtaining a poor quality OCTA image ($P = 0.875, 0.117, 0.531$ and 0.136 , respectively). After the implementation of a multivariable model, older age ($P < 0.001$), male gender ($P = 0.045$), worse MD ($P < 0.001$), absence of eye tracking technology ($P < 0.001$), and image type ($P < 0.001$) remained significantly associated with a higher likelihood of capturing a poor quality OCTA image. (Table 4) Similar results were found for factors that were associated with poor quality image for each scan type. (Supplemental Table 2)

Prevalence of artifacts

The majority of images with acceptable QS had no artifacts (76.6%) while the prevalence of having one artifact and two or more artifacts was 13.6% and 9.8%, respectively. Eye movement artifact was the most common type of artifact detected in the OCTA images with acceptable QS (10.6%), followed by defocus (9.6%), correctable (7.6%) and uncorrectable (5.4%) segmentation error. The prevalence of different subtypes of artifacts in each image type is illustrated in Table 5.

A separate analysis by diagnostic groups revealed eye movement, defocus and segmentation error artifacts to be the most prevalent subtypes of artifacts in OCTA images. While segmentation error was the most prevalent subtype of artifact in images of glaucoma (15.7%) and glaucoma suspect (11%) eyes, eye movement artifact was the most frequently detected artifact in images obtained from healthy eyes (5.5%). A detailed description of the prevalence of different subtypes of artifacts is presented in Supplemental Table 3.

HD image type had a similar likelihood of having poor quality (OR = 0.93, $P = 0.384$) comparing to non-HD image type. However, after reviewing images with an acceptable QS, HD image was associated with a lower likelihood of having at least one severe artifact comparing to non-HD image type (OR = 0.81, $P = 0.036$). Images that were taken from the ONH area had a lower likelihood of having poor quality comparing to those captured from the macular area (OR = 0.52, $P < 0.001$). Also, in the subgroup of images with acceptable QS, ONH images were associated with a lower likelihood of having at least one severe artifact comparing to macular images (OR = 0.74, $P = 0.001$).

Images obtained from the ONH area were associated with a higher likelihood for the presence of shadow (OR = 1.55, $P = 0.004$), defocus (OR = 1.28, $P = 0.032$), segmentation error (OR = 1.40, $P = 0.001$) and Z offset (OR = 3.80, $P < 0.001$) artifacts and a lower likelihood for the presence of eye movement (OR = 0.18, $P < 0.001$) artifact comparing to those obtained from the macular area. HD image type was associated with a higher likelihood for the presence of eye movement (OR = 1.29, $P = 0.05$) and a lower likelihood for the presence of decentration (OR = 0.43, $P < 0.001$) artifact. (Supplemental Table 4)

Figure 2 shows the proportion of images with no artifact, one artifact and 2 or more artifacts across different QS in images with QS of 4 to 10. Higher QS was associated with a consistent trend of decreasing prevalence of artifacts from the QS of 4 to 10.

Separate subanalyses at two levels of last scans for each visit and last scan during the follow up revealed similar results for the proportion of poor quality images (Supplemental Table 5) and the characteristics associated with increased likelihood of capturing poor quality images (Supplemental Tables 6 and 7).

Effect of severe artifacts on the global metrics of OCTA images

Eighty-five pairs of OCTA images were included for this sub-analysis. The average percentage of variation among all pairs of OCTA images was 8% (95% CI: 7%, 10%). Thirty eight percent of the pairs showed a percentage of variation $\geq 10\%$ indicating that there is more than a 10% change in the global vessel density measurements between the poor quality and the good quality OCTA images after recapture. Figure 3 shows 2 examples of poor quality OCTA images that were retaken with the intent to minimize the influence of artifacts on the quantitative OCTA measurements. The difference in global vessel density is compared between the poor quality and the good quality images in each pair.

Classification accuracy of QS and SSI

The classification accuracy of QS and SSI to detect good quality images among images with acceptable QS was analyzed using receiver operating characteristic curves (ROCs). The area under the ROC curves (AUROCs) of QS and SSI for discriminating between good quality and poor quality images were 0.65 (95% CI: 0.62, 0.69) and 0.70 (95% CI: 0.68, 0.73), respectively (Figure 4). Among images with acceptable QS, sensitivity and specificity of automated OCTA quality measures to identify good quality OCTA images were 88% and 42% for QS ≥ 6 and 84% and 43% for SSI ≥ 55 , respectively. Sensitivity analysis for different levels of QS and SSI to identify good quality OCTA images is provided in Supplemental Table 8 and Figure 4.

Discussion

In this study, we evaluated different types of OCTA artifacts present in the superficial retinal layer in a large sample of healthy, glaucoma suspect, and glaucoma participants. As many as one-fourth of OCTA images with acceptable QS were affected by at least one severe artifact that interferes with the interpretability of the scan. Furthermore, patient ocular characteristics, scan type and implementation of eye tracking technology were associated with the presence of different types of artifacts and the overall qualification of OCTA images.

The importance of characterization and identification of image artifacts in accurate clinical interpretation of OCTA images cannot be overstated. Previous studies have mainly focused on evaluating the repeatability of quantitative OCTA measures like vessel density and FAZ¹⁸⁻²¹. However, the validity of such indices can generally be affected by the presence of different types of artifacts leading to a poor quality image. Our study showed one-third of the captured OCTA images do not have acceptable quality necessary for using the

quantitative measurements such as vessel density in clinical practice and research. Even among images with acceptable QS, about one-fourth of the OCTA images had poor quality due to the presence of severe artifacts.

The prevalence of severe OCTA artifacts associated with the quality of OCTA images was inconsistent in previous studies.^{21–23, 30} Holmen et al.²¹ evaluated 406 OCTA images of diabetic retinopathy patients and reported the overall prevalence of severe artifacts to be 50%. On the other hand, Enders et al.²³ found that only 9% of OCTA images of a heterogeneous clinical group of patients were affected with severe artifacts, that hindered the interpretability of the microvascular structure. Inconsistency in defining the types and severity of artifacts and difference in the experience of the technicians acquiring images and clinical status of study participants may account for part of the observed differences in the prevalence of artifacts. It is noteworthy to mention that in the current study, 40% of OCTA images in the glaucoma group had poor quality compared to 15% in the healthy group so that patient and disease characteristics also influence the ability to acquire good quality images. These findings emphasize the importance of patient and technician education to increase the quality of the OCTA images.

Individual demographic and ocular factors affect the likelihood of obtaining good quality OCTA images. Older age and male gender were associated with a higher likelihood of capturing poor quality images. Older patients may have more difficulty staying focused on a fixed target during the OCTA image acquisition. Higher frequency of media opacities such as cataract and age-related pathologies of the retina may be other contributing factors to the increased prevalence of poor quality images in this group. Furthermore, glaucoma eyes were twice as likely to have poor quality images compared to normal eyes of the same age. This is in line with previous studies suggesting the increased prevalence of severe image artifacts leading to poor quality images in eyes with pathological conditions.^{22, 30} This may be the result of failure of the OCTA software algorithms developed on normal retinal structure to process the captured images from diseased tissues.⁹ Of note, the odds of incorrect automatic segmentation of the retinal superficial layer in a glaucoma eye was twice that of a normal eye even after adjustment for age and visual field MD. In addition, increasing disease severity (defined by visual field MD) resulted in an increased prevalence of poor quality images. Retinal thickness declines with the disease progression of glaucoma patients.^{31, 32} This causes a decrease in signal intensity of the reflected waves from retinal tissue and decreases the signal/noise ratio; leading to increased likelihood of OCTA artifacts and poor quality images. Thus, instrument provided quantitative OCTA measurements like vessel density should be interpreted only after detailed review of the images, especially in patients with late stage glaucoma.

The present study showed that scan type was associated with the likelihood of obtaining good quality OCTA images. Our results indicate that HD images were associated with a lower likelihood for the presence of severe artifacts than non-HD images. Gathering more reflection data points from retinal tissue leads to increased horizontal, vertical and axial resolution of the initial OCTA volumetric data. In turn, this increases the signal/noise ratio and the likelihood of obtaining images without artifacts. With the advent of faster OCTA machines, more data points can be obtained during a limited time of scan capture and this

has the potential to further increase the quality of OCTA images. Moreover, the proportion of good quality images was higher in ONH images than that in macular images. A probable explanation for the higher proportion of poor quality images in the macula may be a lower performance of OCTA image processing algorithms for images that are obtained from this area especially when the signal intensity is low. This warrants improvement in the newer versions of the OCTA instrument software.

The introduction of eye tracking technology has increased the likelihood of obtaining good quality OCTA images and has reduced the prevalence of severe artifacts. The duration of OCTA scan acquisition is longer than other eye imaging modalities and patients are required to fixate on a constant target during this time. Involuntary eye movements may happen, especially in older patients with retinal pathology, that lead to erroneous pixel densities manifesting as artifacts. Accordingly, built-in hardware and software have been developed to address this issue. Our results show that the odds of acquiring a poor quality image after using the eye tracking technology is half that without using this technology. The prevalence of eye movement and defocus artifacts were significantly reduced while there was no reduction in the prevalence of segmentation artifact after the implementation of eye tracking technology. This confirms the ability of this technology to compensate for some degree of eye movement during scan capture.

General quantitative quality measures are limited in their ability to detect artifacts and poor quality OCTA images. With the cut-off values of QS ≤ 6 and SSI > 55 , the specificity of detecting poor quality images is around 40%. Thus, about 60% of poor quality images are above both thresholds. This can be partly explained by the fact the QS and SSI are not designed to assess artifacts such as eye movement, decentration, segmentation error, and Z-offset. Rather, QS is calculated based on the assessment of focus motion and signal strength, and SSI is calculated based only on overall signal strength, the average of backscattered light during scanning of the entire scan and may not pick up localized weak signals. Furthermore, both QS and SSI are influenced by media opacity, quality of the cornea surface the thickness of the RNFL. Our findings are in line with those found by Holmen et al. that showed the limitation of automated quality measures to detect good quality OCTA images in patients with diabetic retinopathy.²¹ Accordingly, manual scan review is a necessary step to ensure that good quality OCTA images are used to evaluate patients in studies and clinical settings. To further improve the algorithms generating quality measurements, different types of artifacts and ocular pathologies that affect the structure must be taken into consideration when developing automated quality assessment metrics.

Although this is the largest study evaluating the prevalence of artifacts and the ocular and patient characteristics associated with increased likelihood of obtaining poor quality OCTA images, there are some limitations. First, because of the previous evidence on the relevance of the superficial retinal layer microvasculature to the structural changes observed in glaucoma,^{8, 27, 28} we focused on the identification and characterization of OCTA artifacts in this layer. Thus, our findings do not describe the prevalence of OCTA artifacts related to the deeper retinal layers such as projection artifacts. Second, we adhered to a rigorous protocol in data acquisition and evaluation.³³ Our study population was selected from a cohort study with a robust design²⁴ and the images were acquired by experienced technicians and

manually reviewed by expert observers. The true prevalence of artifacts associated with a higher likelihood of capturing poor quality OCTA images can be influenced by the expertise of the operators and compliance of the patients. Accordingly, we expect the prevalence of poor quality images to be higher in real-world scenarios. Correctable factors like poor centration of an image and unintentional blink or head movement of a patient may influence the quality of ophthalmic images at the time of acquisition. Technicians and practitioners are familiar with many of these factors and often reacquire the images to reduce the magnitude of these artifacts. In this study, however, we analyzed all of the captured images to provide a closer estimation to the true prevalence of OCTA artifacts in routine clinical and research settings. However, in a sub-analysis including the last image of each visit which may reflect a repeat scan by the operator to overcome a previous poor quality scan, we showed a similar proportion of poor quality captured images. Our study evaluated scans with QS values of 4 or higher, which is more liberal than the manufacturer's recent recommendation of 6. With this protocol, advanced glaucoma eyes can be included that otherwise would be excluded due to the thin retinal nerve fiber/superficial layer and resulting lower signal intensity and therefore lower QS. The manufacturer's proposed cut-off of QS = 6 had a sensitivity of 88% and specificity of 42% to identify good quality OCTA images. Lastly, the potential influence of different degrees of media opacity on the quality of OCTA images could not be evaluated. Further studies are needed to assess the optimal cut-offs for different subtypes of OCTA artifacts and characterize the artifacts associated with other ocular pathologies and their impact on the quantitative outputs of the OCTA software such as vessel density measurements.

In conclusion, the present study shows that artifacts associated with an increased likelihood of obtaining poor quality OCTA images are frequent. Individual demographic and ocular conditions affect the presence of such artifacts. Given the likelihood of a high prevalence of poor quality OCTA images, one should not rely solely on the quantitative assessments that are provided automatically by OCTA instruments. To ensure appropriate interpretation of OCTA images, they should be systematically reviewed to identify artifacts. Moreover, OCTA images should be reacquired whenever an apparent and correctable artifact is present on a captured image.

Supplementary Material

Refer to Web version on PubMed Central for supplementary material.

Acknowledgement:

Financial Support: National Institutes of Health/National Eye Institute Grants EY029058, EY011008, EY027510, EY026574, and Core Grant P30EY022589; UC Tobacco Related Disease Research Program (T31IP1511); an Unrestricted Grant from Research to Prevent Blindness (New York, NY); Topcon; and participant retention incentive grants in the form of glaucoma medication at no cost from Alcon Laboratories Inc., Allergan, Akorn, and Pfizer Inc.

Abbreviations and Acronyms:

CCT central corneal thickness

CI	confidence interval
DIGS	diagnostic innovations in glaucoma study
HD	high density
HIPPA	Health Insurance Portability and Accountability Act
IOP	intraocular pressure
MD	mean deviation
OCT	optical coherence tomography
OCTA	optical coherence tomography angiography
ONH	optic nerve head
PSD	pattern standard deviation
QS	quality score
RNFL	retinal nerve fiber layer
ROC	receiver operating characteristic
SD-OCT	spectral domain optical coherence tomography
SSADA	split-spectrum amplitude decorrelation angiography
SSI	signal strength index
UCSD	University of California, San Diego
VF	visual field

References:

1. Spaide RF, Klancnik JM Jr, Cooney MJ. Retinal Vascular Layers Imaged by Fluorescein Angiography and Optical Coherence Tomography Angiography. *JAMA ophthalmology*2015;133:45–50. [PubMed: 25317632]
2. De Carlo TE, Romano A, Waheed NK, Duker JSJ. vitreous. A review of optical coherence tomography angiography (OCTA). 2015;1:5.
3. Chalam K, Sambhav KJ. research v. Optical coherence tomography angiography in retinal diseases. 2016;11:84.
4. Yarmohammadi A, Zangwill LM, Diniz-Filho A, et al. Optical Coherence Tomography Angiography Vessel Density in Healthy, Glaucoma Suspect, and Glaucoma Eyes. *Investigative Ophthalmology & Visual Science*2016;57:OCT451-OCT459.
5. Rao HL, Pradhan ZS, Weinreb RN, et al. Regional Comparisons of Optical Coherence Tomography Angiography Vessel Density in Primary Open-Angle Glaucoma. *American Journal of Ophthalmology*2016;171:75–83. [PubMed: 27590118]
6. Yarmohammadi A, Zangwill LM, Diniz-Filho A, et al. Peripapillary and Macular Vessel Density in Patients with Glaucoma and Single-Hemifield Visual Field Defect. *Ophthalmology*2017;124:709–719. [PubMed: 28196732]

7. Yarmohammadi A, Zangwill LM, Diniz-Filho A, et al. Relationship between Optical Coherence Tomography Angiography Vessel Density and Severity of Visual Field Loss in Glaucoma. *Ophthalmology* 2016;123:2498–2508. [PubMed: 27726964]
8. Moghimi S, Zangwill LM, Pentado RC, et al. Macular and optic nerve head vessel density and progressive retinal nerve fiber layer loss in glaucoma. 2018;125:1720–1728.
9. Spaide RF, Fujimoto JG, Waheed NK. IMAGE ARTIFACTS IN OPTICAL COHERENCE TOMOGRAPHY ANGIOGRAPHY. *Retina* 2015;35:2163–2180. [PubMed: 26428607]
10. Ray R, Stinnett SS, Jaffe GJ. Evaluation of image artifact produced by optical coherence tomography of retinal pathology. *American Journal of Ophthalmology* 2005;139:18–29. [PubMed: 15652824]
11. Han IC, Jaffe GJ. Evaluation of Artifacts Associated with Macular Spectral-Domain Optical Coherence Tomography. *Ophthalmology* 2010;117:1177–1189.e4.
12. Asrani S, Edghill B, Gupta Y, Meerhoff G. Optical coherence tomography errors in glaucoma. *J Glaucoma* 2010;19:237–242. [PubMed: 19661819]
13. Asrani S, Essaid L, Alder BD, Santiago-Turla C. Artifacts in spectral-domain optical coherence tomography measurements in glaucoma. *JAMA ophthalmology* 2014;132:396–402. [PubMed: 24525613]
14. Liu Y, Simavli H, Que CJ, et al. Patient Characteristics Associated With Artifacts in Spectralis Optical Coherence Tomography Imaging of the Retinal Nerve Fiber Layer in Glaucoma. *American Journal of Ophthalmology* 2015;159:565–576.e2.
15. Giani A, Cigada M, Esmaili DD, et al. Artifacts in automatic retinal segmentation using different optical coherence tomography instruments. 2010;30:607–616.
16. Ho J, Sull AC, Vuong LN, et al. Assessment of artifacts and reproducibility across spectral- and time-domain optical coherence tomography devices. 2009;116:1960–1970.
17. Sull AC, Vuong LN, Price LL, et al. Comparison of spectral/Fourier domain optical coherence tomography instruments for assessment of normal macular thickness. 2010;30:235.
18. Conti FF, Young JM, Silva FQ, Rodrigues EB, Singh RP, Jos, Lasers, Retina I. Repeatability of split-spectrum amplitude-decorrelation angiography to assess capillary perfusion density within optical coherence tomography. 2018;49:e9–e19.
19. Magrath GN, Say EAT, Sioufi K, Ferenczy S, Samara WA, Shields CLJR. Variability in foveal avascular zone and capillary density using optical coherence tomography angiography machines in healthy eyes. 2017;37:2102–2111.
20. Rim JH, Lee S-T, Gee HY, et al. Accuracy of next-generation sequencing for molecular diagnosis in patients with infantile nystagmus syndrome. 2017;135:1376–1385.
21. Holmen IC, Konda MS, Pak JW, et al. Prevalence and Severity of Artifacts in Optical Coherence Tomographic Angiograms. *JAMA ophthalmology* 2019.
22. Ghasemi Falavarjani K, Al-Sheikh M, Akil H, Sadda SR. Image artefacts in swept-source optical coherence tomography angiography. *Br J Ophthalmol* 2017;101:564–568. [PubMed: 27439739]
23. Enders C, Lang GE, Dreyhaupt J, Loidl M, Lang GK, Werner JU. Quantity and quality of image artifacts in optical coherence tomography angiography. *PLOS ONE* 2019;14:e0210505.
24. Sample PA, Girkin CA, Zangwill LM, et al. The african descent and glaucoma evaluation study (ADAGES): Design and baseline data. 2009;127:1136–1145.
25. Sample PA, Girkin CA, Zangwill LM, et al. The African Descent and Glaucoma Evaluation Study (ADAGES): design and baseline data. *Arch Ophthalmol* 2009;127:1136–45. [PubMed: 19752422]
26. Jia Y, Tan O, Tokayer J, et al. Split-spectrum amplitude-decorrelation angiography with optical coherence tomography. 2012;20:4710–4725.
27. Takusagawa HL, Liu L, Ma KN, et al. Projection-Resolved Optical Coherence Tomography Angiography of Macular Retinal Circulation in Glaucoma. *Ophthalmology* 2017;124:1589–1599. [PubMed: 28676279]
28. Liu L, Edmunds B, Takusagawa HL, et al. Projection-Resolved Optical Coherence Tomography Angiography of the Peripapillary Retina in Glaucoma. *American Journal of Ophthalmology* 2019;207:99–109. [PubMed: 31170389]

29. Zhang M, Hwang TS, Campbell JP, et al. Projection-resolved optical coherence tomographic angiography. 2016;7:816–828.
30. Say EA, Ferenczy S, Magrath GN, Samara WA, Khoo CT, Shields CLJR. Image quality and artifacts on optical coherence tomography angiography: comparison of pathologic and paired fellow eyes in 65 patients with unilateral choroidal melanoma treated with plaque radiotherapy. 2017;37:1660–1673.
31. Harwerth RS, Wheat JL, Fredette MJ, Anderson DR. Linking structure and function in glaucoma. Progress in Retinal and Eye Research 2010;29:249–271. [PubMed: 20226873]
32. Medeiros FA, Zangwill LM, Bowd C, Vessani RM, Susanna R, Weinreb RN. Evaluation of retinal nerve fiber layer, optic nerve head, and macular thickness measurements for glaucoma detection using optical coherence tomography. American Journal of Ophthalmology 2005;139:44–55. [PubMed: 15652827]
33. Yarmohammadi A, Zangwill LM, Diniz-Filho A, et al. Optical coherence tomography angiography vessel density in healthy, glaucoma suspect, and glaucoma eyes. 2016;57:OCT451-OCT459.

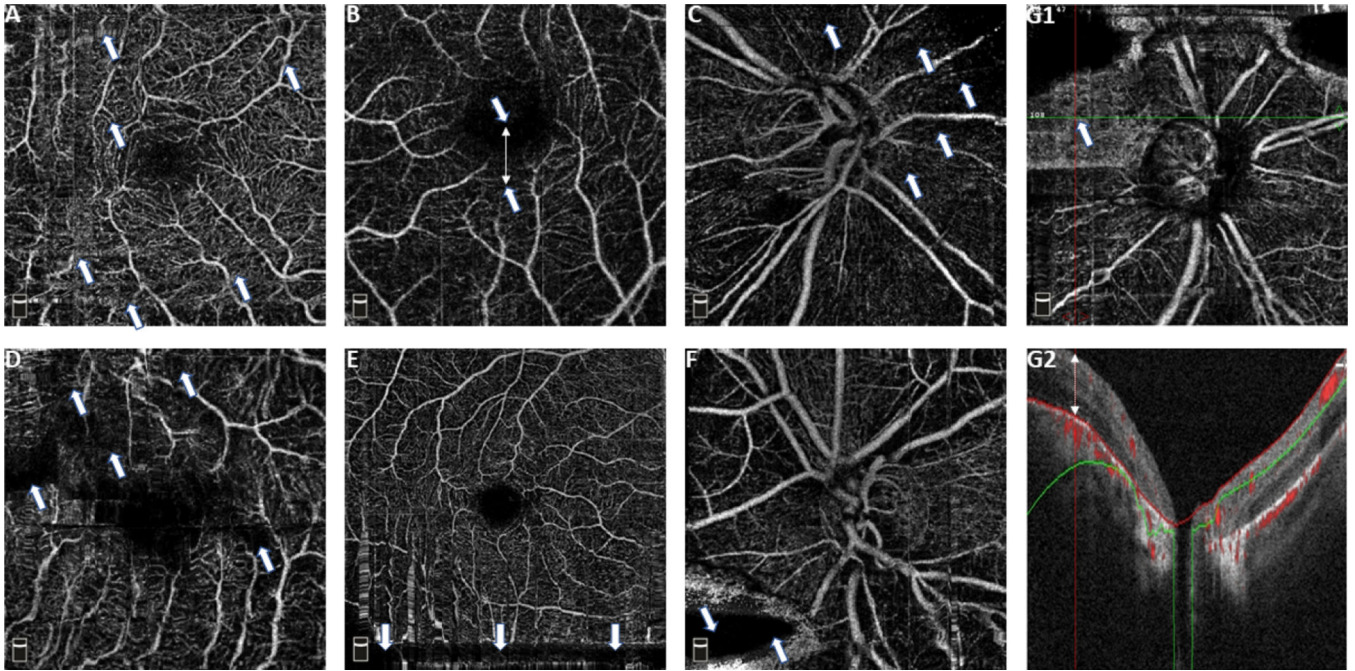


Figure 1.

Examples optical coherence tomography angiography artifacts. A: Eye movement (arrows show horizontal and vertical disruptions in the patterns of microvasculature that can be distinguished as white narrow or stretched lines on the en-face angiogram), B: Decentration (arrows show a displacement in the center of macula from the center of the image), C: Defocus (arrows show areas of decreased visibility of microvascular pattern), D: Shadow (arrows show areas of decreased signal as a result of media opacity), E: Blink (arrows show the course of a black horizontal line resulting from a blink during image acquisition), F: Z offset (arrow shows a loss in image data resulting from the corresponding B-scans falling out of the capture window), G1: Segmentation error en-face image (arrow shows an area with distorted hyperdense microvascular pattern that is not consistent with the adjacent areas), and G2: Segmentation error B-scan (This image shows one of the B-scans corresponding to the territory with segmentation error on G1. The white arrow shows a displaced segmentation line).

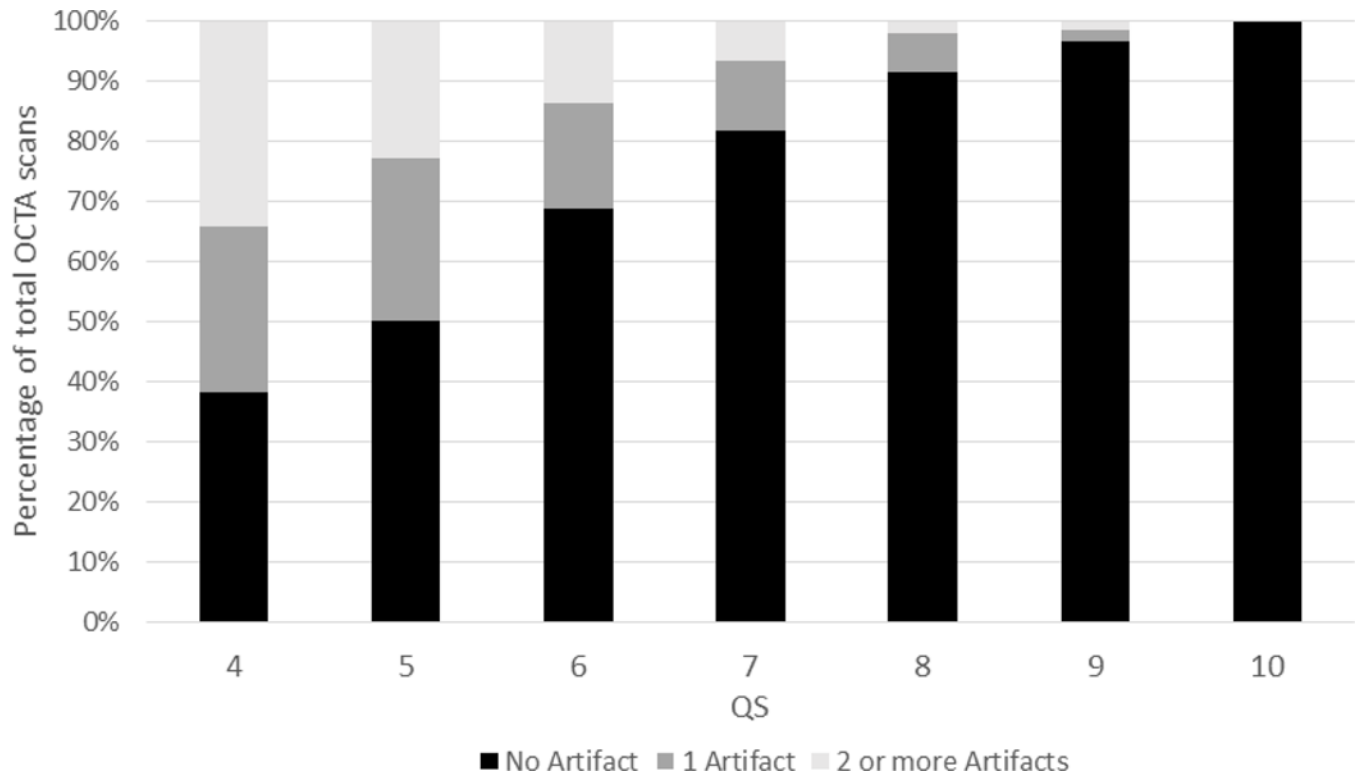


Figure 2.
Prevalence of artifacts among different quality score (QS) categories.

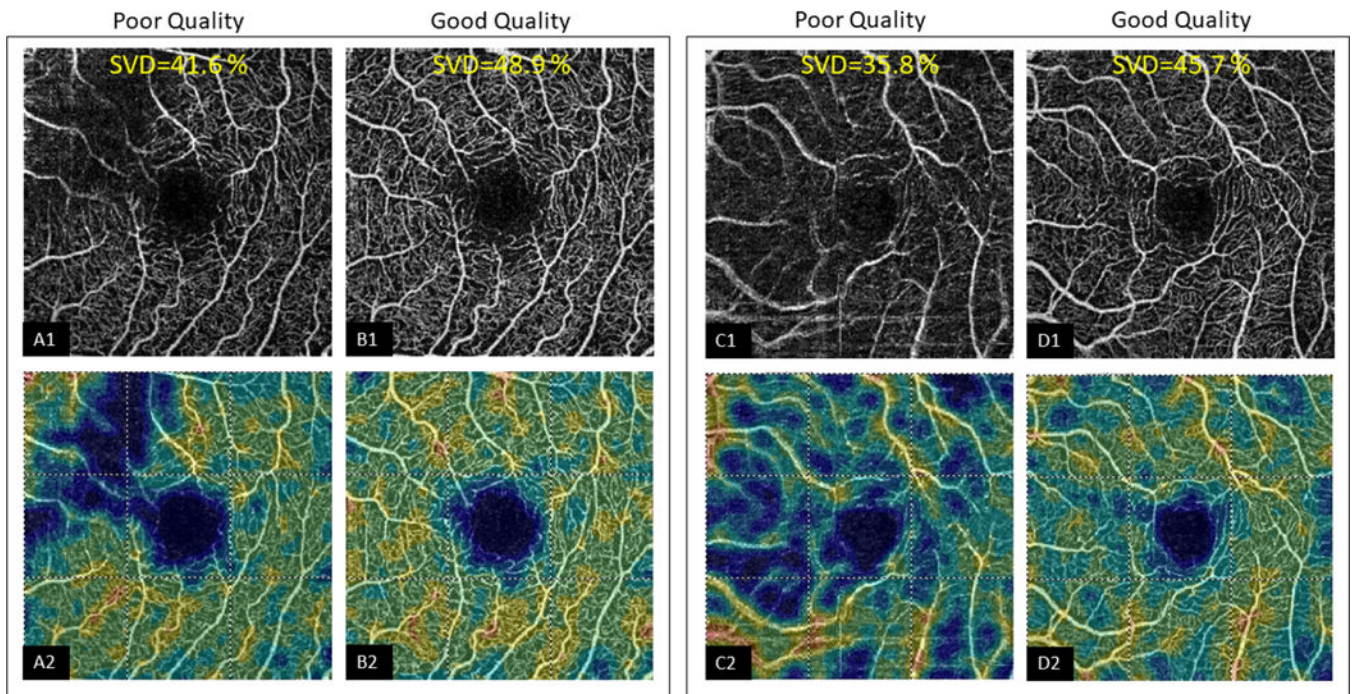


Figure 3.

Two pairs of poor quality (A and C) and good quality (B and D) OCTA en-face images (A1-D1, on the top row) and their respective en-face heatmaps (A2-D2, on the bottom row) are shown. The first pair shows a poor quality macular image with a large shadow artifact affecting the left upper quadrant (A1) and its corresponding influence on vessel density heatmap (A2). The corresponding good quality images are shown in B1 (en-face angiogram) and B2 (en-face heatmap) after image recapture with artifact removal that resulted in a change in macular superficial vessel density (SVD) from 41.6% to 48.9%. Similarly, another sample of a macular image with mixed defocus and eye movement artifacts are shown in C1 and C2 with their corresponding good quality images shown in D1 and D2. Image recapture with the intent to remove the artifacts resulted in a change in SVD from 35.8% to 45.7%.

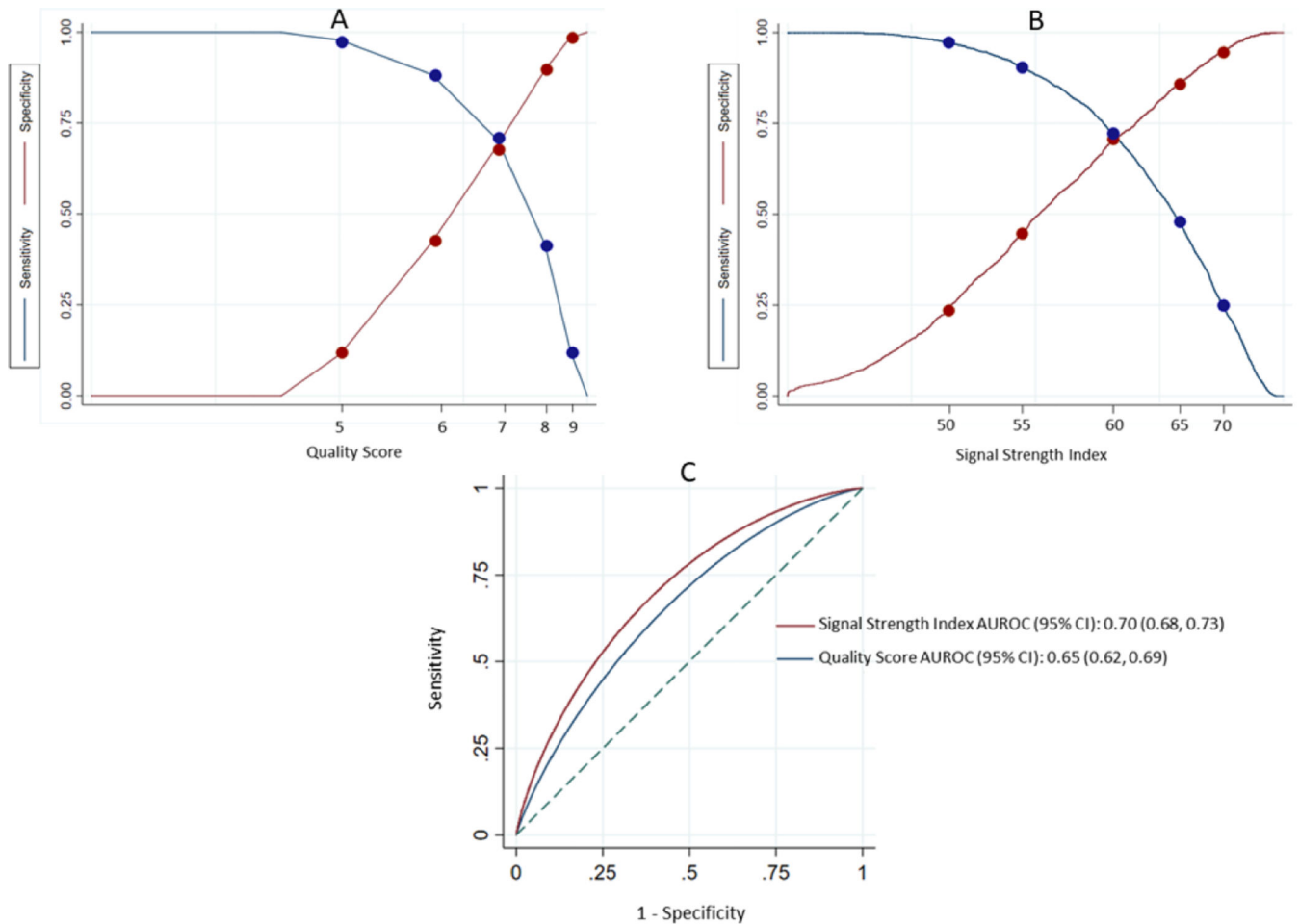


Figure 4.

A: Sensitivity and specificity plots of different quality score cut-offs to detect good quality OCTA images among those with acceptable quality score (QS). B: Sensitivity and specificity plots of different signal strength index cut-offs to detect good quality images among those with acceptable QS. C: Area Under the Receiver Operating Characteristic Curve (AUROC) of QS [blue curve] and signal strength index (SSI) [red curve] for detecting good quality OCTA images among those with acceptable QS.

Table 1.

Definition of Artifacts

Artifact	Definition
Eye movement	Thin horizontal or vertical white lines leading to loss of integrity of the vessels on the en-face angiogram in conjunction with interruption, displacement, doubling or ghosting of vessels, and/or quilting defect. This type of artifact can result in duplication or removal of some parts of retinal vessels from the scan. This artifact was classified as severe if it affected more than 10% of the total B-scans comprising the en-face angiogram.
Defocus	Decrease in reflective intensity and clear visualization of the details of small vessels on the angiogram. Mostly results from decreased reflectance intensity scores in the entire B-scans comprising the angiogram. This artifact was classified as severe if it affected more than 10% of the total B-scans comprising the en-face angiogram.
Shadow	Decreased intensity of retinal layers in isolated areas, often owing to vitreous floaters or corneal opacities. As a result, these structures cannot be clearly visualized and are replaced with dark areas in the en-face angiogram. This artifact was classified as severe if it affected more than 10% of the total B-scans comprising the en-face angiogram.
Decentration	Translocation of the center of the optic nerve head (ONH) or macula from the center of the en-face angiogram to the periphery of the scan. The OCTA algorithm may or may not be able to correctly identify the new center of the ONH or macula. This artifact was classified as severe if it resulted in loss of more than 10% in any adjacent retinal sectors of the ONH or macula.
Segmentation error	Erroneous identification of the borders of superficial vascular layer by the automated segmentation algorithm resulting in a deviation of more than 50% of the total thickness diameter in a B-scan. This artifact was classified as severe if it was observed in more than 10% of total B-scans comprising the en-face angiogram.
Blink	Total loss of reflectance intensity in an area of adjacent B-scans because of a blink during the scan capture. It results in horizontal or vertical black lines on the en-face angiogram. This artifact was classified as severe if it affected more than 5% of the total B-scans comprising the en-face angiogram.
Z offset	Loss of the peripheral borders of B-scans (obtained in both horizontal and vertical raster pattern) due to malalignment of head position during scan capture. This type of artifact happens if the display of a B-scan falls out of the operator window for scan acquisition while capturing the scan. This artifact was classified as severe if it affected more than 5% of the total B-scans comprising the en-face angiogram.

Table 2.

Demographics and Ocular Characteristics of the Study Population

Variables	Healthy (Subjects=63, Eyes=116)	Glaucoma suspect (Subjects=61, Eyes=165)	Glaucoma (Subjects=244, Eyes=368)	P-value *
Baseline Age (years)	54.4 (50.3, 58.5)	68.2 (65.3, 71.0)	73.3 (72.0, 74.6)	< 0.001 †
Gender (Female, %)	40 (63.5%)	40 (65.6%)	124 (50.8%)	0.043 †
Race (African American, %)	17 (27.9%)	8 (13.1%)	60 (24.6%)	0.106 †
Baseline IOP (mmHg)	14.76 (14.13, 15.38)	17.19 (16.44, 17.94)	13.51 (12.95, 14.08)	< 0.001 ‡
Baseline CCT (µm)	549.00 (541.99, 556.02)	550.84 (544.18, 557.51)	539.09 (534.60, 543.58)	0.517 ‡
Baseline axial length (mm)	23.95 (23.77, 24.13)	23.86 (23.69, 24.04)	24.07 (23.95, 24.19)	0.935 ‡
Baseline spherical Refractive Error (D)	-1.07 (-1.44, -0.70)	-0.76 (-1.05, -0.46)	-0.96 (-1.14, -0.77)	0.601 ‡
Baseline cylindrical Refractive Error (D)	0.57 (0.43, 0.72)	0.86 (0.72, 0.99)	1.02 (0.92, 1.11)	< 0.001 ‡
Baseline spherical Equivalent of Refraction (D)	-0.80 (-1.17, -0.43)	-0.33 (-0.63, -0.03)	-0.45 (-0.63, -0.27)	0.368 ‡
Baseline VF MD (dB)	-0.38 (-0.63, -0.13)	-0.71 (-1.13, -0.29)	-6.68 (-7.37, -5.99)	< 0.001 ‡
Baseline VF PSD (dB)	1.67 (1.57, 1.78)	1.95 (1.80, 2.10)	6.08 (5.68, 6.47)	< 0.001 ‡

IOP: intraocular pressure, CCT: central corneal thickness, D: diopter, VF: visual field, MD: mean deviation, PSD: pattern standard deviation

Results are shown in mean (95% confidence interval) for numerical variables and No. (%) for categorical variables.

Generalized linear mixed model was used to compare continuous variables across different diagnostic categories.

Chi square's test was used to compare categorical variables across different diagnostic categories.

* P-values with statistical significance (< 0.05) are shown in bold.

† Analysis was done at the patient level. In case of different diagnoses for right and left eyes, patients were assigned to the group with worse diagnosis.

‡ Analysis was done at the eye level.

Table 3.

Differences between the Characteristics of Good Quality and Poor Quality Images

Variable	Good quality	Poor quality	P-value *
	N = 3478 (66.1%)	N = 1785 (33.9%)	
Age (years)	68.4 (68.0, 68.9)	75.6 (75.1, 76.1)	< 0.001
Gender (Female, %)	1952 (56.1%)	811 (45.4%)	0.037
Race (African American, %)	878 (25.4%)	455 (25.5%)	0.875
IOP (mmHg)	15.10 (14.94, 15.26)	13.90 (13.65, 14.16)	0.042
CCT (μ m)	542.10 (540.69, 543.51)	535.18 (533.12, 537.24)	0.008
Axial length (mm)	24.06 (24.02, 24.10)	23.98 (23.92, 24.04)	0.117
Spherical Refractive Error (D)	-1.10 (-1.17, -1.03)	-0.85 (-0.93, -0.76)	0.531
Cylindrical Refractive Error (D)	0.83 (0.80, 0.86)	0.99 (0.95, 1.04)	0.002
Spherical Equivalent of Refraction (D)	-0.69 (-0.76, -0.62)	-0.35 (-0.43, -0.27)	0.136
VF MD (dB)	-3.29 (-3.46, -3.13)	-6.38 (-6.70, -6.07)	< 0.001
VF PSD (dB)	3.99 (3.87, 4.10)	5.61 (5.42, 5.79)	< 0.001
Diagnosis			< 0.001
Healthy	554 (15.9%)	109 (6.1%)	
Glaucoma suspect	992 (28.5%)	328 (18.4%)	
Glaucoma	1932 (55.6%)	1348 (75.5%)	
QS	7.11 (7.07, 7.15)	4.55 (4.46, 4.64)	< 0.001
SSI	63.92 (63.62, 64.22)	52.44 (51.77, 53.10)	< 0.001

IOP: intraocular pressure, CCT: central corneal thickness, D: diopter, VF: visual field, MD: mean deviation, PSD: pattern standard deviation, QS: quality score, SSI: signal strength index.

Results are shown in mean (95% confidence interval) for continuous and No. (%) for categorical variables.

Generalized linear mixed model was used to compare the characteristics of good quality and poor quality images.

* P-values with statistical significance (< 0.05) are shown in bold.

Table 4.

Univariable and multivariable generalized linear mixed model analysis of the characteristics associated with the increased likelihood of having a **poor quality**OCTA image

Variables	Univariable Model		Multivariable Model	
	Odds ratio (95% CI)	<i>P</i> -value*	Odds ratio (95 % CI)	<i>P</i> -value*
Age (per 10-year increase)	2.00 (1.73, 2.32)	< 0.001	1.84 (1.58, 2.15)	< 0.001
Gender (Female/Male)	0.64 (0.43, 0.97)	0.037	0.69 (0.48, 0.99)	0.045
Race (African American/non-African American)	1.04 (0.64, 1.69)	0.875		
IOP (per 1 mmHg increase)	0.97 (0.95, 1.00)	0.042	0.99 (0.97, 1.02)	0.689
CCT (per 10 µm increase)	0.94 (0.90, 0.99)	0.008	0.96 (0.93, 1.00)	0.067
Axial length (per 1 mm increase)	0.89 (0.76, 1.03)	0.117		
Spherical Refractive Error (per 1 D increase)	1.03 (0.94, 1.14)	0.531		
Cylindrical Refractive Error (per 1 D increase)	1.35 (1.12, 1.63)	0.002	1.07 (0.90, 1.28)	0.464
Spherical Equivalent of Refraction (per 1 D increase)	1.08 (0.98, 1.19)	0.136		
VF MD (per 1-dB decrease)	1.10 (1.07, 1.12)	< 0.001	1.08 (1.05, 1.10)	< 0.001
VF PSD (per 1-dB increase)	1.11 (1.07, 1.15)	< 0.001		
Diagnosis		< 0.001		
Glaucoma suspect/Healthy	2.13 (1.19, 3.80)	0.011		
Glaucoma/Healthy	4.65 (2.74, 7.89)	< 0.001		
Eye Tracking (Tracking/No Tracking)	0.57 (0.48, 0.68)	< 0.001	0.54 (0.45, 0.65)	< 0.001
Image type		< 0.001		< 0.001
3×3 mm ² non-HD macula/4.5×4.5 mm ² non-HD ONH	2.91 (2.38, 3.55)	< 0.001	2.91 (2.36, 3.59)	< 0.001
6×6 mm ² non-HD macula /4.5×4.5 mm ² non-HD ONH	1.36 (1.08, 1.71)	0.010	1.32 (1.04, 1.69)	0.025
4.5×4.5 mm ² HD ONH /4.5×4.5 mm ² non-HD ONH	1.16 (0.90, 1.49)	0.259	1.16 (0.89, 1.51)	0.272
6×6 mm ² HD macula /4.5×4.5 mm ² non-HD ONH	1.68 (1.31, 2.15)	< 0.001	1.72 (1.33, 2.24)	< 0.001

IOP: intraocular pressure, CCT: central corneal thickness, VF: visual field, MD: mean deviation, PSD: pattern standard deviation, D: diopter, HD: high density, ONH: optic nerve head.

* *P*-values with statistical significance ($P < 0.05$) are shown in bold.

Table 5.

Distribution of Artifacts among Image Types (N [%])

Scan type	QS < 4	Artifact types among images with QS = 4							Artifact frequency among images with QS = 4			
		Shadow	Eye movement	Defocus	Segmentation error		Decentration	Blink	Z offset	No artifacts	1 artifact	> 1 artifact
					MC	UnC						
Optic Nerve Head												
Non-HD	113 (8.2)	86 (6.8)	31 (2.5)	130 (10.3)	99 (7.8)	116 (9.2)	65 (5.1)	14 (1.1)	30 (2.4)	983 (77.7)	157 (12.4)	126 (10.0)
HD	63 (8.3)	41 (5.9)	56 (8.0)	83 (11.9)	49 (7.0)	34 (4.9)	14 (2.0)	16 (2.3)	16 (2.3)	554 (79.4)	72 (10.3)	72 (10.3)
Macula												
3×3 mm² non-HD	288 (19.8)	41 (3.5)	243 (20.8)	125 (10.7)	52 (4.5)	45 (3.9)	62 (5.3)	16 (1.4)	5 (0.4)	810 (69.3)	221 (18.9)	138 (11.8)
6×6 mm² non-HD	124 (13.8)	49 (6.4)	81 (10.5)	66 (8.6)	85 (11.0)	26 (3.4)	26 (3.4)	4 (0.5)	9 (1.2)	608 (78.8)	94 (12.2)	70 (9.1)
6×6 mm² HD	134 (17.4)	28 (4.4)	71 (11.2)	30 (4.7)	62 (9.8)	22 (3.5)	17 (2.7)	5 (0.8)	5 (0.8)	523 (82.2)	72 (11.3)	41 (6.5)
Overall	722 (13.7)	245 (5.4)	482 (10.6)	434 (9.6)	347 (7.6)	243 (5.4)	184 (4.1)	55 (1.2)	65 (1.4)	3478 (76.6)	616 (13.6)	447 (9.8)

N: number, QS: quality score, MC: manually corrected segmentation error, UnC: uncorrected segmentation error, HD: high density.